

# Amplitude modulation measurement of symmetrical microwave power sensor

Wang Debo Liao Xiaoping Tian Tao

(Key Laboratory of MEMS of Ministry of Education, Southeast University, Nanjing 210096, China)

**Abstract:** In order to reduce the mismatch error, a direct current (DC) calibration method is introduced when the modulated microwave signal is measured. The microwave power is input to the left section of the power sensor, and the DC power is input to the right of the power sensor. Due to the existence of parasitic loss and electromagnetic coupling, the microwave power results in a mismatch error. However, the DC power does not have the mismatch error. So the DC power applied in the right section can calibrate the mismatch error of the microwave power in the left section. The calibration factor is measured at different modulation rates and modulation depths. The measurement results show that the carrier frequency is the major factor influencing the measurement results. After calibration, the carrier frequency and the modulation rate have little effect on the output voltage. The frequency response becomes relatively flat in the frequency range up to 20 GHz, and the sensitivity on average is enhanced by about 0.12 mV/dBm. Therefore, the DC calibration method has a certain reference value for the terminal-type microwave power sensor.

**Key words:** amplitude modulation; symmetrical; power sensor; direct current (DC) calibration

The microwave power is one of the most important parameters in microwave power equipment and systems. The thermocouple-based power sensor is one of the most widely used tools for microwave power measurement<sup>[1]</sup>. By far, various structures of microwave power sensors based on thermocouple are introduced<sup>[2-4]</sup>, which are subject to several sources of error. In order to eliminate the errors caused by the thermal losses and to simplify the fabrication process, a novel symmetrical microwave power sensor based on the MEMS technology was reported in Ref. [5]. It is measured in a frequency range up to 20 GHz with an input power in a range from 0 to 80 mW. Over the 80 mW dynamic range, the sensitivity can achieve about 0.2 mV/mW. The relative deviation of the input power in the two sections is below 0.1% for an equal output voltage. The key aspect of this power sensor is that the microwave power measurement is conveniently replaced with the DC power measurement. The structure of the power sensor is shown in Fig. 1(a), and the SEM photo of the power sensor is shown in Fig. 1(b). In the power sensor, the right section has the same CPW, load resistor and thermopile as the left section. It eliminates the

errors caused by thermal losses since the two sections have equal thermal losses. In order to further study the symmetrical microwave power sensor, the amplitude modulation (AM) of an information-bearing microwave signal is measured using the power sensor. There are three basic types of modulations. They are the AM, the frequency modulation (FM) and the phase modulation (PM). The microwave power measurement is independent of frequencies and phases. Therefore, the FM measurement and the PM measurement are ignored. In addition, the AM is widely used<sup>[6-7]</sup> and is being constantly-depth studied<sup>[8-10]</sup> now. So, the AM measurement is mainly studied in this paper.

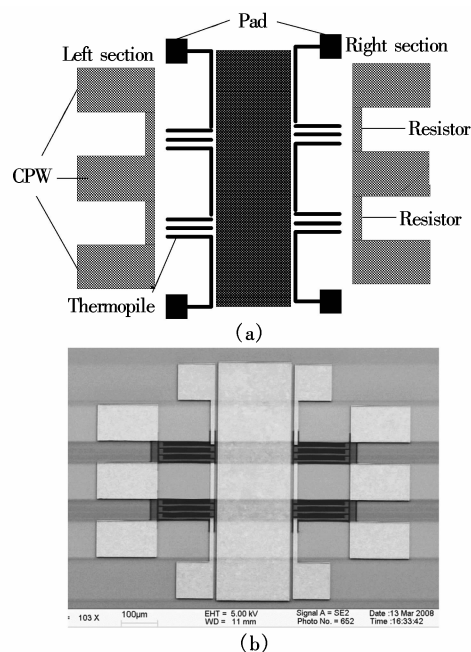


**Fig. 1** Symmetrical power sensor. (a) Structure of the power sensor; (b) SEM photo of the power sensor

## 1 Principle

The principle of the power sensor is based on the differential principle as shown in Fig. 1. The right section of the power sensor has the same CPW, the load resistor and the thermopile as the left section. Since the two sections have equal thermal losses, the error caused by thermal losses can be eliminated. Due to its symmetrical structure, this power sensor provides more accurate microwave power measurement capability without mismatch uncertainty, and it restrains temperature drift. For the AM, the carrier signal is defined as

$$V_c = V_{cm} \cos \omega_c t \quad (1)$$

The modulation signal is defined as

Received 2009-09-18.

**Biographies:** Wang Debo (1983—), male, graduate; Liao Xiaoping (corresponding author), male, doctor, professor, xpliao@seu.edu.cn.

**Foundation items:** The National Natural Science Foundation of China (No. 60976094), the National High Technology Research and Development Program of China (863 Program) (No. 2007AA04Z328).

**Citation:** Wang Debo, Liao Xiaoping, Tian Tao. Amplitude modulation measurement of symmetrical microwave power sensor[J]. Journal of Southeast University (English Edition), 2010, 26(1): 68–72.

$$V_{\Omega} = V_{\Omega m} \cos \Omega t \quad (2)$$

The waveform for the modulated signal after the AM is shown in Fig. 2(a). The modulated signal can be expressed as

$$v_{AM}(t) = V_m(t) \cos \omega_c t = V_{cm} (1 + M_a \cos \Omega t) \cos \omega_c t \quad (3)$$

$$M_a = \frac{k_a V_{\Omega m}}{V_{cm}} = \frac{V_{mmax} - V_{mmin}}{V_{mmax} + V_{mmin}} \leq 1 \quad (4)$$

where  $M_a$  is the modulation depth. The frequency spectral distribution after the AM is shown in Fig. 2(b). The frequency spectral distribution can be expressed as

$$v_{AM} = V_{cm} \cos \omega_c t + \frac{M_a V_{cm}}{2} \cos(\omega_c + \Omega) t + \frac{M_a V_{cm}}{2} \cos(\omega_c - \Omega) t \quad (5)$$

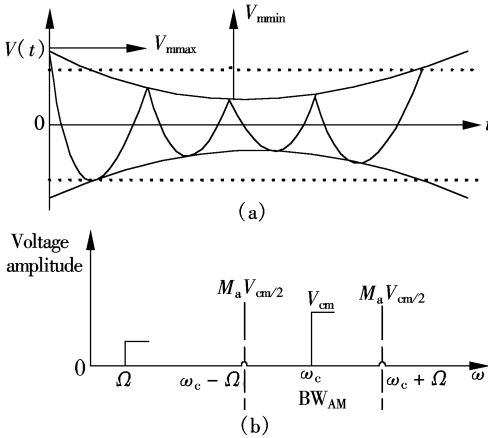


**Fig. 2** Amplitude modulation. (a) Waveform of the modulated signal; (b) Frequency spectral distribution

The total power absorbed by the load after the AM can be expressed as

$$P_L = \frac{V_{cm}^2 (1 + M_a \cos \Omega t)^2}{2R_L} \quad (6)$$

The average power in one cycle can be expressed as

$$P_{av} = \frac{1}{2\pi} \int_0^{2\pi} P_L d\Omega t = P_0 \left( 1 + \frac{M_a^2}{2} \right) = P_0 + P_{SB} \quad (7)$$

where  $P_0 = \frac{V_{cm}^2}{2R_L}$  is the carrier power, and  $P_{SB} = \frac{M_a^2}{2} P_0$  is the double-sideband power. Therefore, the double-sideband power changes with the modulation depth  $M_a$ , which changes the total power. Thus, the modulation depth can influence the output voltage. So the AM measurement of the symmetrical power sensor is studied.

## 2 Simulation

Compared with the right section of the power sensor as shown in Fig. 1(a), the left section has losses caused by the microwave signal. Therefore, the AM measurement error needs to be analyzed. The AM measurement diagram of the left section is shown in Fig. 3.

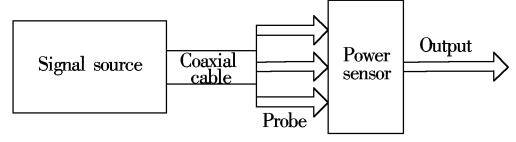


**Fig. 3** Measurement diagram

There is the coaxial cable with the characteristic impedance  $z_0$  between the signal source and the power sensor. When the coaxial cable matches the signal source and the power sensor, the power received by the power sensor equals the output power  $p_G$  of the signal source. In order to perfectly match, the input impedance of the power sensor is required to agree with the characteristic impedance  $z_0$  of the coaxial cable. However, they usually do not agree with each other. So, there exists a reflection coefficient  $\Gamma_L \neq 0$ . Thus, the power measured by the power sensor is the net power  $p_L$  absorbed by the load resistors, which is below the output power  $p_G$  of the signal source. Especially, when the coaxial cable does not match the signal source, it also produces loss between the signal source and the coaxial cable. So, there also exists a reflection coefficient  $\Gamma_G \neq 0$ . Generally, the above two errors are called the mismatch error<sup>[11]</sup>.

According to theoretical analysis and practical experience, the AM measurement error sources can be expressed as follows:

- 1) Mismatch error;
- 2) The thermal loss error such as heat conduction, convection and radiation loss;
- 3) Temperature drift error;
- 4) Signal source error due to unsteadiness;
- 5) Operating error.

Errors 4) and 5) are usually ignored because they influence measurement results little. Due to the differential principle and the symmetrical structure, this symmetrical power sensor eliminates the errors 2) and 3). Therefore, the mismatch error 1) is the main AM measurement error for the symmetrical power sensor which includes the losses of the cable and the probe. The magnitude of the mismatch error is not only determined by the magnitude of  $\Gamma_G$  and  $\Gamma_L$ , but it is also determined by their phases. Due to the fact that it is very difficult to measure the phase relationship, the mismatch error belongs to the uncertain error.

The microwave signal reflected between the signal source and the power sensor is shown in Fig. 4.  $\Gamma_G$  and  $\Gamma_L$  are the reflection coefficients of the signal source and the power sensor, respectively. For the mismatch case, the microwave signal produces multiple reflections between the signal source and the power sensor, and the amplitude and the direction of the first few reflections are shown in Fig. 4.

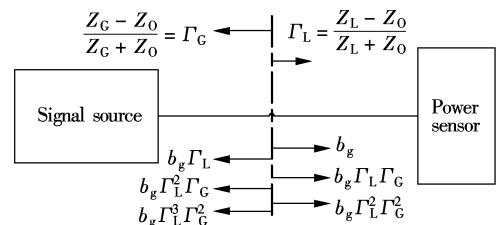


**Fig. 4** Microwave signal reflection

The total amplitude for the incident wave can be expressed as

$$A = b_g + b_g \Gamma_L \Gamma_G + b_g \Gamma_L^2 \Gamma_G^2 + \dots = \frac{b_g}{1 - \Gamma_L \Gamma_G} \quad (8)$$

The total amplitude for the reflected wave can be expressed as

$$B = b_g \Gamma_L + b_g \Gamma_L^2 \Gamma_G + b_g \Gamma_L^3 \Gamma_G^2 + \dots = \frac{b_g \Gamma_L}{1 - \Gamma_L \Gamma_G} \quad (9)$$

where  $|b_g|^2$  represents the output power  $p_0$  of the signal source for the matching. According to Eqs. (8) and (9), for the mismatching, the incident power and the reflected power can be respectively expressed as

$$P_i = |A|^2 = \frac{P_0}{|1 - \Gamma_L \Gamma_G|^2} \quad (10)$$

$$P_r = |B|^2 = \frac{P_0 |\Gamma_L|^2}{|1 - \Gamma_L \Gamma_G|^2} = P_i |\Gamma_L|^2 \quad (11)$$

At this point, the power measured by the power sensor can be expressed as

$$P_L = P_i - P_r = |A|^2 - |B|^2 = \frac{P_0(1 - |\Gamma_L|^2)}{|1 - \Gamma_L \Gamma_G|^2} \quad (12)$$

In addition, the relationship between  $p_0$  and  $p_G$  can be expressed as

$$P_0 = P_G(1 - |\Gamma_G|^2) \quad (13)$$

According to Eq. (13), Eq. (12) can also be expressed as

$$P_L = P_G \frac{(1 - |\Gamma_G|^2)(1 - |\Gamma_L|^2)}{|1 - \Gamma_L \Gamma_G|^2} \quad (14)$$

Therefore, the mismatch error  $\delta$  can be deduced as

$$\delta = \frac{P_G - P_L}{P_G} = 1 - \frac{(1 - |\Gamma_G|^2)(1 - |\Gamma_L|^2)}{|1 - \Gamma_L \Gamma_G|^2} \quad (15)$$

Ignoring the second order small quantities for Eq. (15), the limit range of the mismatch error can be deduced as

$$\delta = \pm 2 |\Gamma_G| |\Gamma_L| \quad (16)$$

Suppose that  $|\Gamma_G| = 0.25$ ,  $|\Gamma_L| = 0.2$ , and  $\delta = \pm 2 \times 0.25 \times 0.2 = \pm 10\%$ . This shows that the AM measurement error caused by the mismatch cannot be ignored.

### 3 Measurement

The AM measurement<sup>[2, 12]</sup> is accomplished with an Agilent E8257D signal generator, a cascade Microtech 1200 probe station, a DC voltage source and two digital voltmeters.

There are four factors which influence the AM measurement. They are the carrier frequency, the carrier amplitude, the AM rate and the AM depth, respectively. For ideal conditions, the AM measurement is independent of the carrier frequency and the AM rate, and it is dependent on the carrier

amplitude and the AM depth. However, according to Eqs. (8) to (16) and to simulation results, the carrier frequency and the AM rate can influence the AM measurement results due to the mismatch error. Therefore, in order to achieve accurate AM measurement, the AM measurement errors must be calibrated. In this paper, the DC calibration method for the microwave power AM measurement is introduced to compensate for the mismatch error.

By comparing with the DC power at 10 dBm for an equal output voltage, the calibration factor for the entire carrier frequency is measured with the AM depth set to 0.5 and the AM rate respectively set to 1, 10, 100 kHz. The measurement result is shown in Fig. 5(a). As shown in Fig. 5(a), the calibration factor increases greatly with the carrier frequency, and increases little with the increase in the AM rate. In order to study the calibration factor varying with the AM depth, the calibration factor is measured with the AM rate set to 10 kHz and the AM depth respectively set to 0.2, 0.5 and 0.8. The measurement result is shown in Fig. 5(b). As shown in Fig. 5(b), the calibration factor increases rapidly with the increase in the carrier frequency, and increases slowly with the increase in the AM depth. Therefore, it is obvious that the carrier frequency is the main factor influencing the mismatch error.

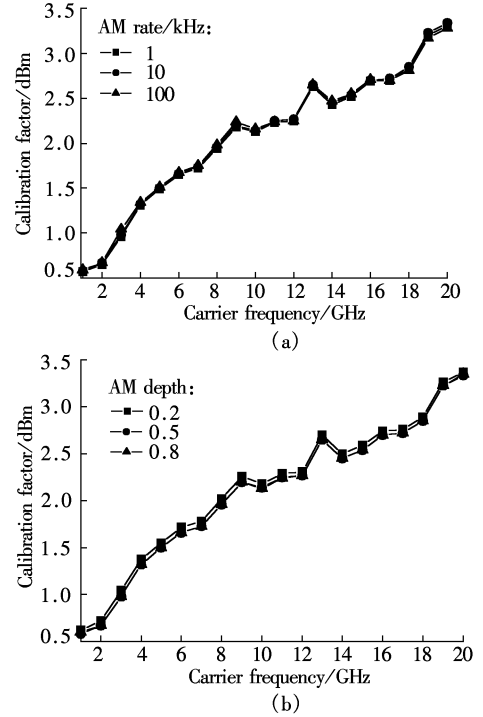


**Fig. 5** Calibration factor varying with AM depth and rate. (a) Varying with the AM rate; (b) Varying with the AM depth

The microwave signals are applied in a left section with the carrier frequency range from 1 to 20 GHz with the AM depth respectively set at 0.2, 0.5 and 0.8. The carrier amplitude and the AM rate are respectively fixed at 10 dBm and 10 kHz. The output voltages before calibration are recorded as shown in Fig. 6. Due to the mismatch error, the output voltage decreases with the decrease in the carrier frequency. According to the calibration factor with the AM rate set at 10 kHz in Fig. 5, the results after calibrations 0.2

(a), 0.5(a) and 0.8(a) are shown in Fig. 6. The frequency response after calibration becomes relatively flat in the frequency range up to 20 GHz, and the sensitivity is enhanced on average by about 0.12 mV/dBm at 1 GHz with the AM depth respectively set at 0.2, 0.5 and 0.8. The higher the carrier frequency is, the more the sensitivity is enhanced. And the sensitivity enhances averagely about 1.3 mV/dBm at 20 GHz. The reason is that the loss power increases with the increase of the carrier frequency. Therefore, the sensitivity is enhanced after calibration.

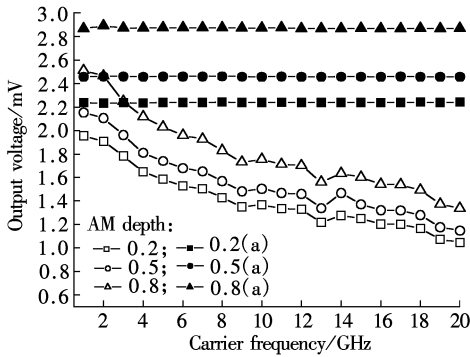


**Fig. 6** Output voltage measured vs. carrier frequency characteristics with different AM depths

In order to further study the output voltage varying with the increase in the AM depth, the carrier frequency and the AM rate are considered respectively as shown in Fig. 7 and Fig. 8. The output voltage increases with the increase in the AM depth, which is to be expected. As analyzed previously, the mismatch error caused by the carrier frequency is larger than that caused

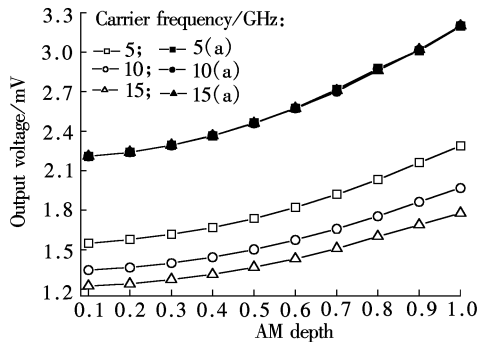


**Fig. 7** Output voltage measured vs. AM depth characteristic with different carrier frequencies

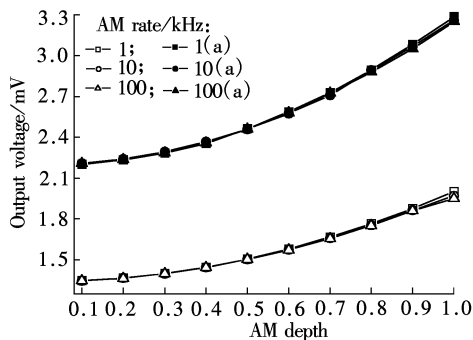


**Fig. 8** Output voltage measured vs. AM depth characteristic with different AM rates

by the AM rate, and the output voltage has little correlation with the carrier frequency and the AM rate after calibration. At the same time, the sensitivity is greatly improved. Therefore, the DC calibration method can be regarded as a reference for calibrating the terminal-type power sensor.

## 4 Conclusion

The AM measurement of the symmetrical microwave power sensor is presented. Due to the symmetrical structure, the power sensor restrains temperature drift. The mismatch error is analyzed and the DC calibration method is introduced to compensate the mismatch error. So the power sensor is created to provide more accurate AM measurement capability. The frequency response after calibration becomes relatively flat in the frequency range up to 20 GHz, and the sensitivity is enhanced on average by about 0.12 mV/dBm.

## References

- [1] Lamy J C. Microelectronics enhances thermocouple power measurements [J]. *Hewlett Packard J*, 1974, **26**(1): 16 – 18.
- [2] Dehe A, Krozer V, Chen B, et al. High-sensitivity microwave power sensor for GaAs-MMIC implementation [J]. *IEEE Electronics Letters*, 1996, **32**(23): 2149 – 2150.
- [3] Milanovic V, Gaitan M, Bowen E D, et al. Thermoelectric power sensor for microwave applications by commercial CMOS fabrication [J]. *IEEE Electron Lett*, 1997, **18**(9): 450 – 452.
- [4] Lalinsky T, Hascik S, Mozolova, Z, et al. The improved performance of GaAs micromachined power sensor micro-system [J]. *Sensors and Actuators A: Physical*, 1999, **76** (1/2/3): 241 – 246.
- [5] Wang Debo, Liao Xiaoping. A novel symmetrical microwave power sensor based on MEMS technology [J]. *Chinese Journal of Semiconductors*, 2009, **30**(5): 054006-1-054006-5.
- [6] Wang Jian, Cui Chen. The modulation and demodulation systems of the signal sideband on the basis of the system view emulate [J]. *Communication Technology*, 2003, **43** (7): 43 – 45. (in Chinese)
- [7] Quan Jingcai, Chen Qijin. Compatible signal sideband system of phase-amplitude modulation [J]. *Journal of South China University of Technology: Natural Science Edition*, 2002, **30**(4): 37 – 39. (in Chinese)
- [8] Bao Changxiang. Analog switch: its application in amplitude modulation and demodulation [J]. *Journal of Neijiang Teachers College*, 2002, **17**(4): 19 – 23. (in Chinese)
- [9] Chen Qijing. Spectrum analysis of phase amplitude modulation [J]. *IEEE Trans on Broadcasting*, 1990, **36**(1): 34 – 36.
- [10] Zhang Guijun, Zhou Wei, Zheng Yanqiu. Affection to phase noise of a CW carrier by the pulse modulation [J]. *Journal of Astronautic Metrology and Measurement*, 2003, **23**(1): 17 – 21. (in Chinese)
- [11] Zhang Wenyuan, Wang Hong, Zheng Jinbin, et al. Effects of microwave power transmission on mismatch errors and measurement accuracy [J]. *Journal of Air Force Radar Academy*, 2005, **19**(4): 34 – 36. (in Chinese)
- [12] Ziemer R E, Tranter W H. *Principles of communications: systems, modulation and noise* [M]. New York: John Wiley & Sons, 2003: 101 – 147.

# 对称式微波功率传感器的幅度调制测量

王德波 廖小平 田 涛

(东南大学 MEMS 教育部重点实验室, 南京 210096)

**摘要:** 为了减小失配造成的测试误差, 在测量调制信号的微波功率时提出了一种直流校正方法. 在传感器左端输入微波功率, 右端输入直流功率, 微波功率存在的寄生损耗和电磁耦合造成了失配误差, 而直流功率不存在失配误差, 所以通过右端输入的直流功率可以校正左端微波功率的失配误差. 测试了在不同调制率和调制深度的校正因子. 测试结果表明, 载波频率是造成幅度调制测试误差的主要因素, 校正后载波频率和调制率对输出电压的影响很小, 频率响应在 20 GHz 范围内变得相对平滑, 而且灵敏度平均提高了大约 0.12 mV/dBm. 因此, 该直流校正方法对于终端式微波功率传感器具有一定的参考意义.

**关键词:** 幅度调制; 对称式; 功率传感器; 直流校正

**中图分类号:** TN402